Electronic Supplementary Material (ESI) for Journal of Materials Chemistry C.

Supporting Information

Combining Two-Photon Photoemission and Transient Absorption Spectroscopy to Resolve Hot Carrier Cooling in 2D Perovskite Single Crystals: the Effect of Surface Layer

Weihua Lin[1, +], Mingli Liang[1,2, +], Yuran Niu[3], Zhesheng Chen[4], Marie Cherasse[4,5], Jie Meng[2], Xianshao Zou[1], Qian Zhao[2], Huifang Geng[6], Evangelos Papalazarou[7], Marino Marsi[7], Luca Perfetti[4], Sophie E. Canton[8,], Kaibo Zheng[1,2,*], Tönu Pullerits[1,*]*

Abstract: We investigate hot carrier (HC) cooling in two-dimensional (2D) perovskite single crystals by applying two complementary ultrafast spectroscopy techniques – transient absorption (TA) and time-resolved two-photon photoemission (TR-2PPE) spectroscopies. TR-2PPE directly maps the hot electron distribution and its dynamics in the conduction band to the detected photoelectron distribution. While TR-2PPE selectively probes the upper layer of the material, TA provides information on the whole bulk. Two cooling regimes are resolved in both techniques. The fast timescale of 100-200 fs is related to the electron scattering by longitudinal optical (LO) phonons and the slow timescale of 3-4 ps corresponds to the LO phonon relaxation. The HC cooling dynamic of TA measurement has faster initial stage and higher starting temperature for the slower stage than in TR-2PPE measurements. Conclusions about spatial sensitivity of the cooling dynamics across the 2D perovskite single crystals constitute valuable information that can guide the future development of HC solar cells and thermoelectric applications based on 2D perovskites.

DOI: 10.1002/anie.2021XXXXX

Table of Contents

Experimental Procedures

Synthesis of 2D Perovskite Single Crystals. The bulk single crystal of $(BA)_2(MA)_{n-1}Pb_nI_{3n+1}$ (n = 1, 2, 3) were obtained by the temperature gradient growth method, which is similar to our previous work.[1] First, PbI_2 (99 %), methanamine hydriodide (98 %, MAI),

butylammonium iodide (98 %, BAI), hypophosphorous acid solution (50 % in water; 5 ml) and hydroiodic acid (57 % in water; 0.25 ml) were initially formulated as the precursor solutions in 20 ml glass bottles (all the chemicals were supplied by Sigma-Aldrich). For the three samples (n = 1, 2 and 3), the PbI_2/MAI/BAI contents are 1.5 mmol/0 mmol/2.0 mmol, 1.5 mmol/1.5 mmol/2.0 mmol, and 1.5 mmol/2.5 mmol/2.0 mmol, respectively. Then, such precursor solutions were sealed and stirred at room temperature for 30 mines. After that, they were heated at 80 °C until solutions become completely clear. The bulk single crystals were grown from the clear solutions at a cooling rate of 0.5 °C/day starting from 55 °C. The obtained crystals and their ball-stick model of the structure are shown in Figure S4. In order to facilitate the measurements of our transient spectra, these bulk single crystals are separated into thin flakes using Scotch tape in a glove box. Later, these 2D perovskite flakes are sealed between the two quartz glasses with liquid optical clear adhesive (without touching samples, see Supporting Information S12) to prevent them from being damaged by moisture or oxidation after being taken out of the glove box.

Position-Selective Transient Absorption (TA) Measurements. The transient absorption (TA) spectra are collected in a transmission configuration with 400 nm pump beam and white light as probe beam. A pulsed laser of 800 nm wavelength, 80 fs pulse duration and 1kHz repetition frequency is generated by injecting the seed laser (Mai Tai, Spectra Physics) into a regenerative amplifier (Spitfire XP Pro, Spectra Physics). The output fundamental laser is split by a beam splitter for generating pump and probe beams. The pump is produced by second harmonic generation of 800nm incident beam *via* a BBO crystal. The probe beam is generated by focusing the 1350nm laser, which is obtained from the 800nm fundamental laser *via* a collinear optical parametric amplifier (TOPAS-C, Light Conversion), on a thin CaF_2 plate that mounted on a moving stage to avoid heat damage. The pump and probe beams are not parallel but is set to spatially overlap on flake sample which is monitored by digital microscope during TA measurements, see Supporting Information S12. The polarization between pump and probe beams is set to the magic angle (54.7°) by using the Berek compensator in the path of pump beam. A circular graduated neutral density filter is also placed in the pump path for the excitation intensity-dependent measurements. The time delay between pump and probe is controlled by a delay stage placed in the path of probe beam. After transmitting through sample, the probe beam is eventually passing the prism and dispersed on the photodiode array. To gain better signal-to-noise, the intensity of the scattering of pump beam is monitored and a gate is set to discard the useless data affected by laser fluctuation. A limit is set how different the scan results can be to alert for the possible degradation-related changes. If the signal (transmitted pulse intensity) differs from the average by more than 10 %, the measurement is stopped and the sample is carefully inspected. The optical microscope figure can be considered as a position reference for locating the suitable flake under digital microscope, where the neighboring bulky crystals work as marks. During the TA measurements, the position of probe light on sample was fixed and it was confirmed by the real-time digital microscope measurements.

Time-Resolved Two-Photon Photoemission (TR-2PPE) Spectroscopy. The TR-2PPE spectra were measured with angle-resolved photoemission spectroscopy (ARPES) in FEMTOARPES lab at SOLEIL synchrotron facility in France.[2] The fundamental laser beam (1.55 eV, 250 kHz repetition rate, 6 μJ intensity) is generated from a Ti:Sapphire laser system (Light conversion). The output fundamental laser is split by a beam splitter for generating pump and probe beams. The pump we applied in this study is the second harmonic generation (3.1 eV with maximum power density of 0.5 mJ/cm^2) of the fundamental one. The probe beams are the third harmonic beam (4.65 eV) in Figure 2 and fourth harmonic beam (6.2 eV) as shown in Figure S16. The probe geometry is set to have a 45° incident angle on the sample. The emitted photo-electrons are collected and analyzed by an electrostatic analyzer in kinetic energy with a resolution of 50 meV. Note that the investigation of electron emission angle is not included in this study. A delay stage is applied to control the time delay between pump and probe with temporal resolution better than 100 fs considering the pulse duration.

The single crystals of 2D perovskite are first exfoliated by a scotch tape to produce to remove the surface residuals. After exfoliated crystal is then pressed onto the copper post in the sample plate, with the other side of crystal is glued on a ceramic post. After being loaded on the sample holder in the manipulator, the crystal is further cleaved by knocking down the ceramic post to have a flat atomic surface free from the moisture or oxygen invasion. The degradation test is carried out on sample using more intense pump beam than what is used in the real experiment. At the highest intensities the signal started to decrease after long time exposure. The experiments shown in the article were carried out at lower intensities and the exposer times were shorter warranting negligible degradation during the measurements.

Low-energy Electron Diffraction (LEED) Measurements. The LEED pattern was measured in a spectroscopic photoemission and low energy electron microscope (SPELEEM III, Elmitec) in MAXPEEM beamline at MAX-IV laboratory in Lund, Sweden. The instrument has a single digit nanometer spatial resolution. Before being placed in the loadlock of the microscope, the surface of the 2D perovskite single crystal was attached on a tape, while the other end of the tape is fixed on the surface of the loadlock. After pumping down the loadlock, the sample holder was taken out from the loadlock by a transfer arm, the tape was then automatically removed from the sample surface. At the same time, a few layers of the sample were peeled off and trashed. By using this method, a cleaved clean surface was obtained. Finally, the sample was transferred quickly into the main chamber that has a base pressure better than 1 x 10^{-10} torr for further analysis.

Results and Discussion

S1. Characterization of 2D perovskite single crystals

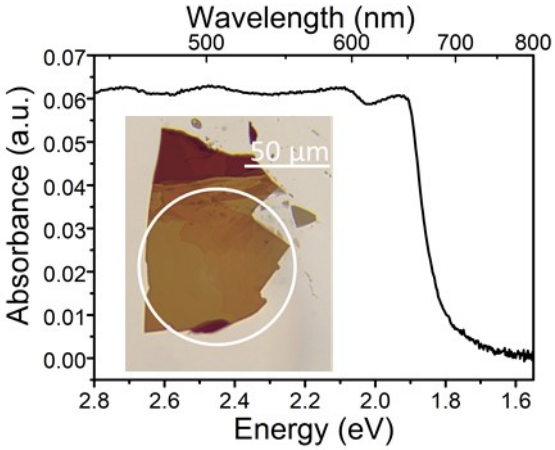

Figure S1. Steady-state absorption spectrum of 2D perovskite bulk crystal and the optical microscope image of 2D perovskite flake on quartz with the thickness around 100 nm.

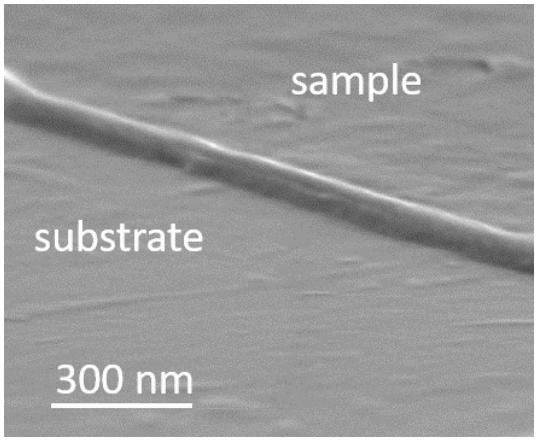

Figure S2. Tilted scanning electron microscope (SEM) measurements of 2D perovskite flake which shares similar contrast in optical microscope measurements (*i.e.*, similar thickness) to the analyzed samples.

Since the purity plays an important role in the advance spectroscopy measurements, as the flake for transient absorption (TA) measurements has only few hundred nanometers thickness and x-ray measurements are surface-sensitive, we conduct the TA measurements on other 2D perovskite flakes that have different n-value as common impurities in single phase 2D perovskite films. By comparing the signal positions in Figure S3, we can confirm the high purity of the 2D perovskite flakes and that the flake fabrication method is suitable for providing clean samples with suitable thickness. In the meantime, it indicates the feasibility of fitting temperature of HC based on transient absorption spectra of 2D perovskite flakes, as the signal from sample can be clearly assigned without being affected by other phases.

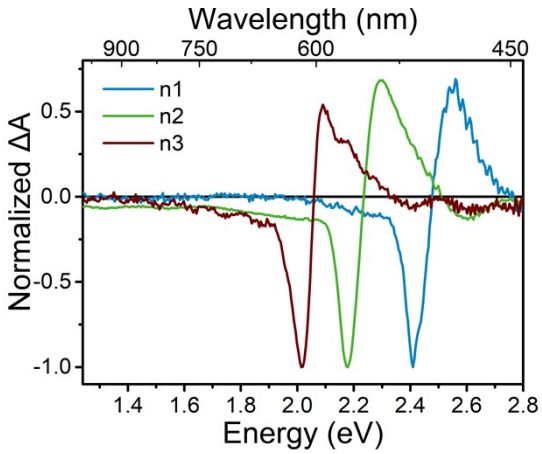

Figure S3. TA spectra of 2D perovskite with different n-value in $(BA)_2(MA)_{n-1}Pb_nI_{3n+1}$ (n = 1, 2 and 3) at 1 ps time delay, pumped with 400 nm excitation with medium intensity (around 15 uJ/cm^2 per pulse).

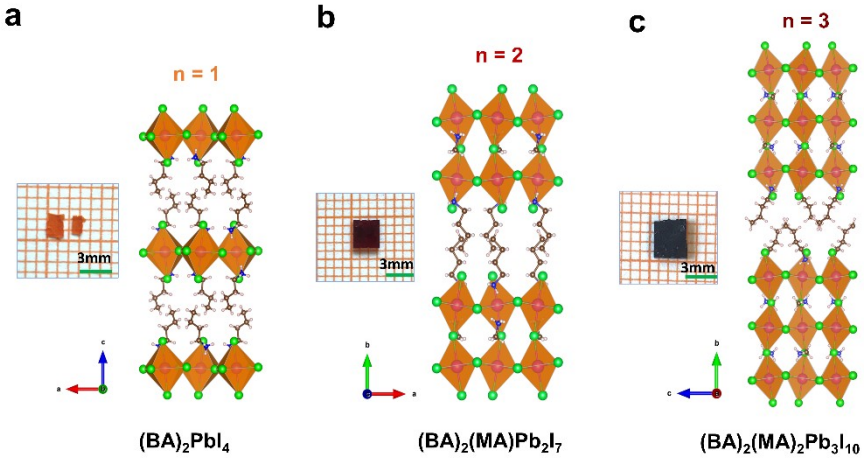

Figure S4. The bulk single crystals and their ball-stick model of (a) $(BA)_2PbI_4$ (n1), (b) $(BA)_2(MA)Pb_2I_7$ (n2), and (c) $(BA)_2(MA)_2Pb_3I_{10}$ (n3).

S2. Absorption coefficient and carrier density calculations of 2D perovskite flake

The 2D perovskite single crystal thick flake (not the thin flake that we investigated hot carrier cooling dynamics in) was first fabricated on the quartz, as shown in Figure S5 using the same method described in S1. The optical density (OD) at 400 nm is 1.2, obtained by measuring the remaining percentage of transmitted light. The area size difference between the sample (2.7×10^4 um^2) and the white light beam (1.125×10^5 um^2) was considered in the calculation. The influence of scattering and reflectance from sample are corrected by calculating the loss of transmittance at 1000 nm, as 83% of beam can be collected *via* this bulk sample at the same detection angle, comparing to the incident light intensity.

$$A = log_{10}(I_0/I) \quad (1)$$

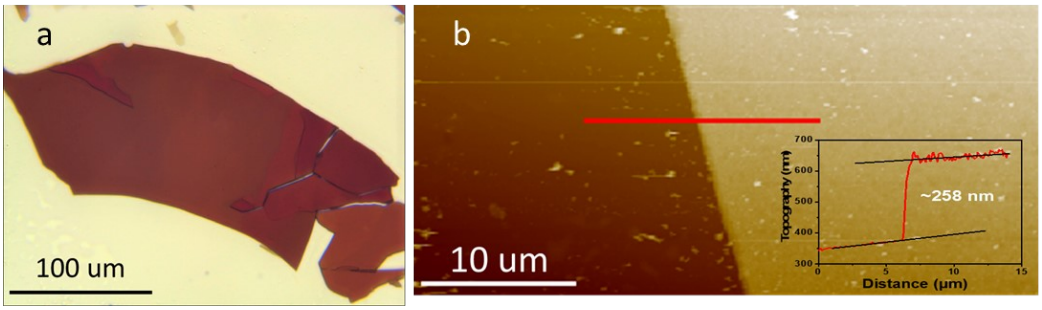

Figure S5. (a) Optical microscope image of a 2D perovskite thick flake on quartz and (b) atomic force microscope (AFM) measurement on it where the red line indicates the measured path on sample.

We can obtain the absorption coefficient ε ~1.0×10^5 cm^{-1}, where the d is the length of light path inside the crystal and is equal to the thickness of the thick flake as 258 nm, see Figure S5 (b).

$$\varepsilon = 2.303 \times A/d \quad (2)$$

The excitation density n can be calculated as $n = f \times \varepsilon$, where the f is the photon flux in photons per cm^2. The excitation intensities used in the TA measurements are summarized as Table S1.

Table S1. Excitation density at different photon flux per pulse

Energy density I ($\mu J/cm^2$/pulse)	Photons flux f (ph/cm^2/pulse)	Excitation density n (ph/cm^3/pulse)
7	1.4×10^{13}	1.4×10^{18}
15	3.0×10^{13}	3.0×10^{18}
30	6.0×10^{13}	6.0×10^{18}
60	1.2×10^{14}	1.2×10^{19}
120	2.4×10^{14}	2.4×10^{19}

S3. Absorption coefficient of 2D perovskite thin film

To confirm the absorption coefficient of 2D perovskite, the thin film has also been measured. As for the absorption in 700 nm region, it is due to the 2D perovskite with higher *n*-value which have narrower band gap. The other *n*-value 2D perovskite in film sample is so-far unavoidable. This is one of the reasons why we use in our experiments flakes from a single crystal with well-defined *n* as is confirmed in the Figure S3. The absorbance of 2D perovskite film at 400 nm is measured as 1.72, as shown in Figure S6. The absorption coefficient is calculated as $\varepsilon = 2.08\times10^5$ cm^{-1}, where the length of light path inside the thin film is 190 nm measured with profilometer. The calculated absorption coefficient of thin film is on the same order of the single crystal thick flake and prove the validity of calculation in S2.

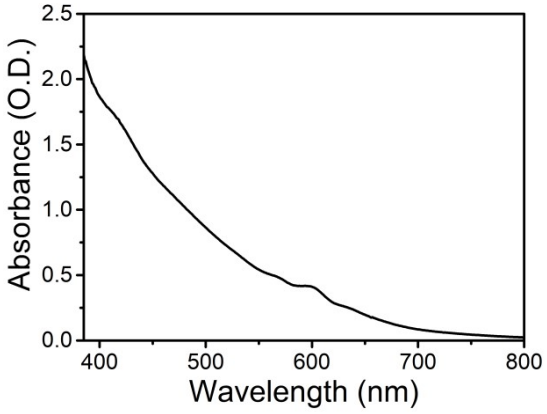

Figure S6. Steady state absorption spectrum of 2D perovskite thin film.

S4. Determination of energy window and offset for TA analysis

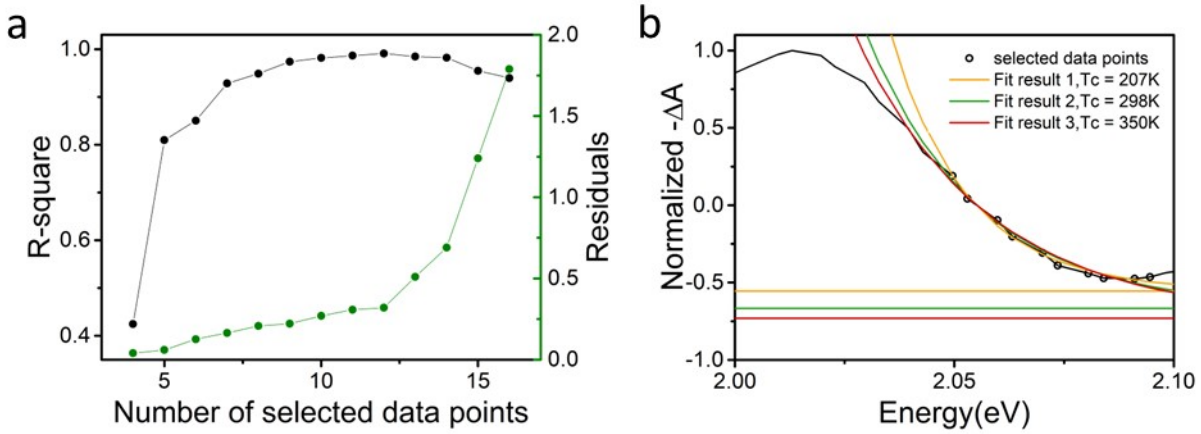

Figure S7. (a) R-square and the sum of absolute value of residuals for spectra fitting with different energy range with equation shown as below. (b) The hot carrier temperature with different offset with 10 data points selected, where result 1 is obtained without restriction while offset is fixed for obtaining result 2 and 3.

The equation used in Figure S7 is

$$\frac{\Delta T}{T} = A_1 + A_2 exp\left(-\frac{E - E_f}{k_B T_c}\right) \tag{3}$$

where the offset is a constant as used in main body.

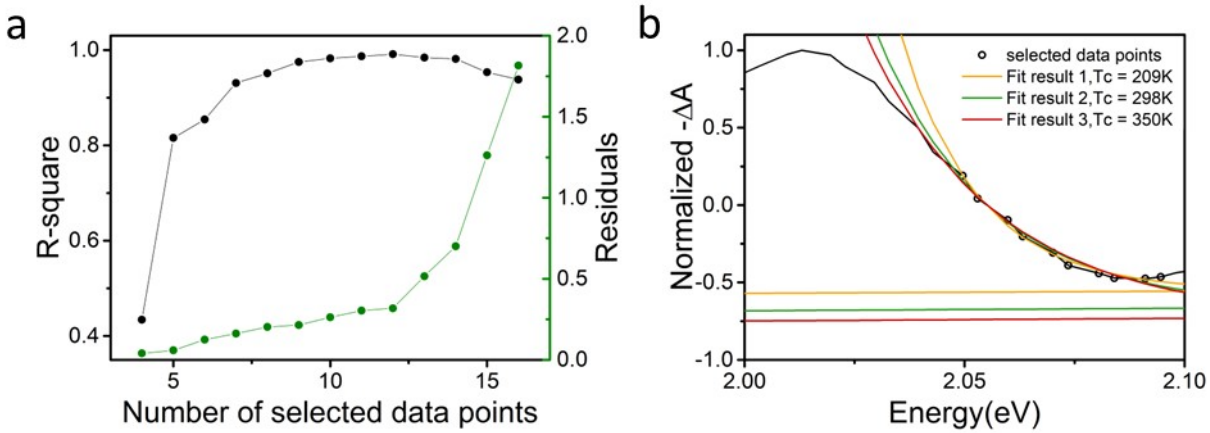

Figure S8. (a) R-square and the sum of absolute value of residuals for spectra fitting with different energy range with equation shown as below. (b) The hot carrier temperature with different offset with 10 data points selected, where result 1 is obtained without restriction while offset is fixed for obtaining result 2 and 3.

The equation used in Figure S8 is

$$\frac{\Delta T}{T} = A_1 E^{-\frac{1}{2}} + A_2 exp\left(-\frac{E - E_f}{k_B T_c}\right) \quad (4)$$

where the parabolic approximation is considered in the first term.

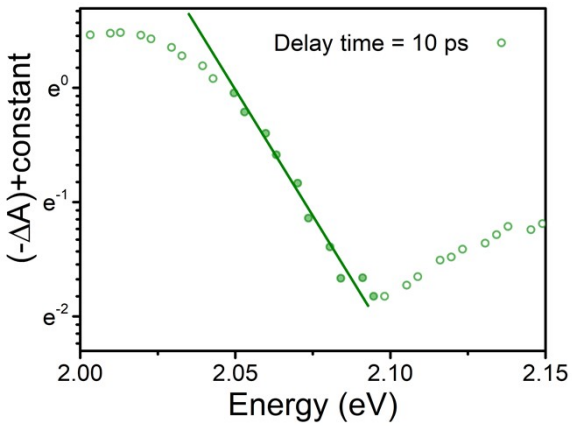

Figure S9. Transient absorption spectrum of 2D perovskite with excitation intensity of 30 μJ/cm^2 at 10 ps delay time. The constant is chosen to make the plot has positive value for log-scale Y-axis. The solid dots are the selected data points for fitting the carrier temperature.

The Y-axis is in the log scale and the deviated data points from the line are not suitable for exponential fitting. In TA analysis, the carrier temperature is obtained by fitting the high energy tail with the Boltzmann distribution exp(-E/k_B*T), therefore the energy window is selected as the solid dot regime.

S5. Quasi-equilibrium timescale

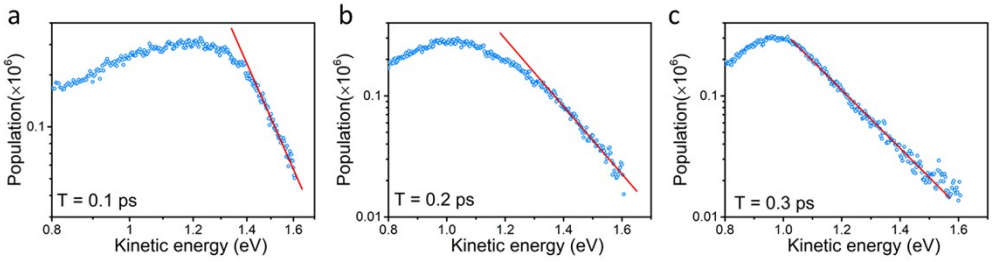

Figure S10. Time-resolved two-photon photoemission (TR-2PPE) spectra at (a) 0.1 ps, (b) 0.2 ps and (c) 0.3 ps, where the pump is 3.1 eV and the probe is 4.65 eV. The Y-axis is in log-scale for clearly showing the high energy tail can be fitted with one exponential component at 0.3 ps.

Figure S10 shows that the population of photoelectrons start to exhibit Boltzmann distribution (*i.e.*, the high energy tail can be fitted with single exponential function) after 0.3 ps.

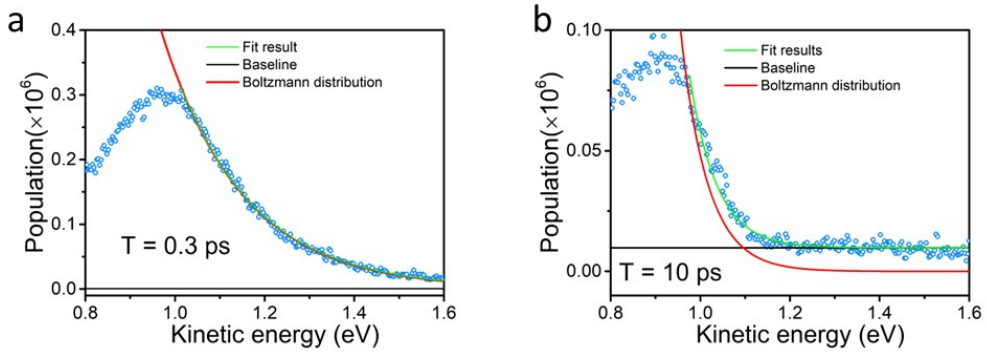

Figure S11. Fitting the TR-2PPE spectra with Boltzmann distribution at (a) 0.3 ps and (b) 10 ps, where the pump is 3.1 eV and the probe is 4.65 eV.

Figure S11 shows that the high energy tail of TR-2PPE spectra can be fitted with Boltzmann distribution. The analysis shows that if we set the hot electron temperature at 10 ps to be 135 K, then at 0.3 ps the temperature of hot electrons is around 1530 K, which is comparable to the result we obtained from average excess energy analysis.

S6. Excitation dependent TA spectra and time dependent HC temperature

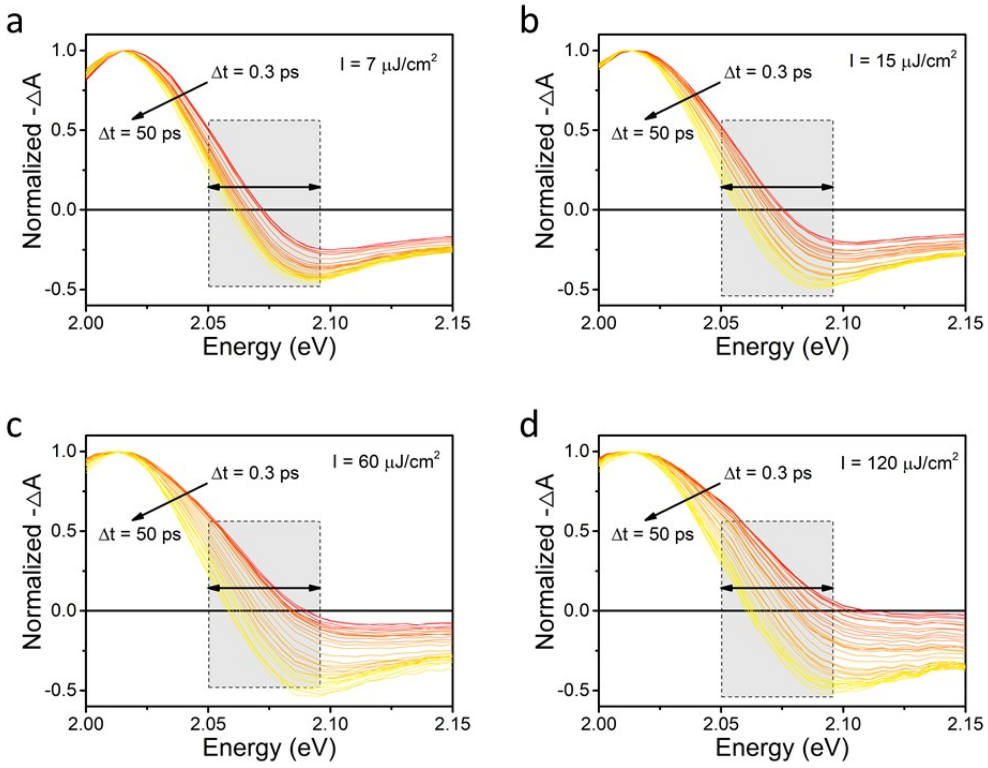

Figure S12. TA spectra of 2D perovskite flake with 400 nm at different intensity of (a) 7 μJ/cm^2, (b) 15 μJ/cm^2, (c) 60 μJ/cm^2 and (d) 120 μJ/cm^2, respectively.

Table S2. Comparison of time delays from initial HC temperature cooled to 600 K in 3D perovskite and our result in 2D perovskite.

Ref	Excess energy (eV)	Carrier density (×10^{19})	Initial carrier temperature (K)	Time until 600 K (ps)
Fu et al. [3]	≈ 0.8	≈ 1.02	≈ 900	≈ 0.8
Yang et al. [4]	≈ 1.45	≈ 1.2	≈ 920	≈ 2
Our result	≈ 1.1	≈ 1.2	≈ 722	≈ 1.5

S7. Comparison to other flakes

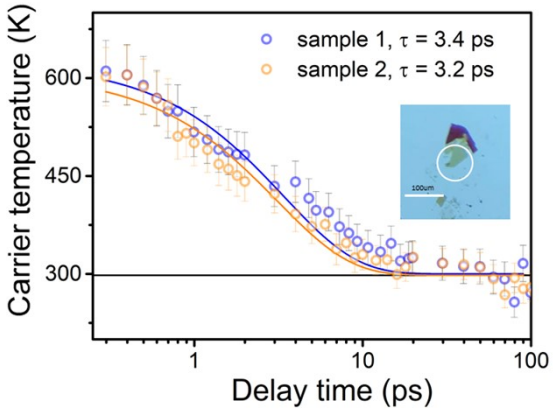

Figure S13. Comparison in HC cooling dynamics with another flake sample (sample 2) under 3.1 eV (400 nm) excitation at intensity of 30 μJ/cm^2.

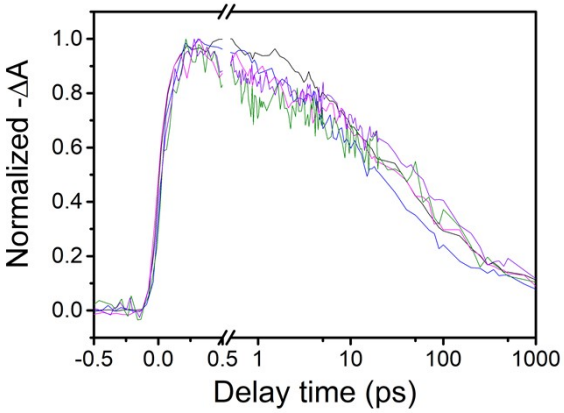

Figure S14. Normalized GSB dynamics (around 610 nm) of 5 different flakes with similar thickness under 3.1 eV (400 nm) excitation at intensity around 15 μJ/cm^2.

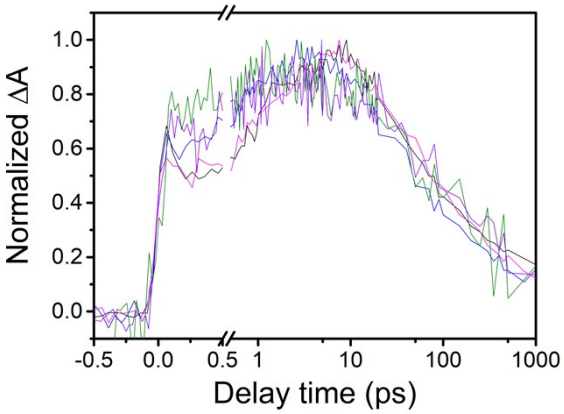

Figure S15. Normalized PIA dynamics (around 590 nm) of 5 different flakes with similar thickness under 3.1 eV (400 nm) excitation at intensity around 15 μJ/cm^2.

S8. Time dependent energy distribution curve (EDC) of TR-2PPE measurements

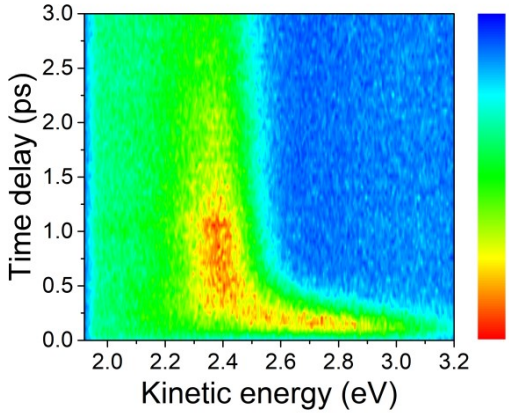

Figure S16. Time-dependent EDC pumped with 3.1 eV of 160 μJ/cm^2 and probed with 6.2 eV. Before measurements, the sample was cooled with liquid N_2 in the main chamber at 4.6 E-11 mbar for slowing the heat damage on samples.

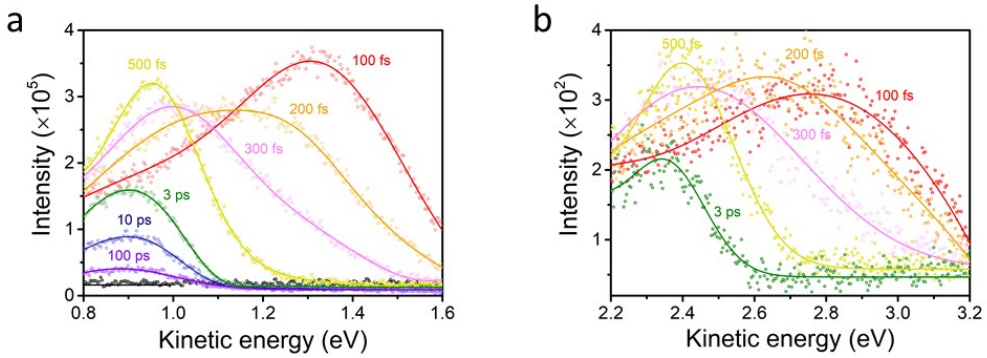

Figure S17. TR-2PPE spectra at selected time delay, where the pump is 3.1 eV and the probe is (a) 4.65 eV or (b) 6.2 eV, respectively. The black line in (a) represents the spectrum at a negative time delay.

In both measurements, the hot electron population at the high excess energy states peak around 100 fs, and then the peak shift to lower excess energy and peak around 3 ps. The similarity indicates the probe energy has not significantly affected the intrinsic hot electron relaxation.

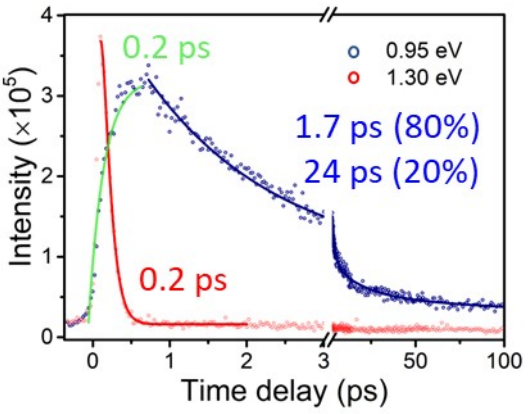

Figure S18. Exponential fitting on the dynamics at different excess energy states (1.30 eV as excess energy state E* 1 and 0.95 eV as excess energy state E* 2) in TR-2PPE measurement.

At early delays the probe pulse creates an intense distribution of hot electrons with excess energy E* 1 peaked at 1.30 eV. After an instantaneous rise to the maximum intensity (Figure S18, red curve), the kinetics of electrons at E* 1 can be fitted by a single-exponential decay with a lifetime of 0.2 ± 0.1 ps. Simultaneously, a broader band with lower excess energy E* 2 peaked around 0.95 eV appears with the rising time (0.2 ± 0.1 ps) matching well with the decay of the E* 1 band. This indicates that the energy of initial photoexcited electrons (E* 1band) is redistributed to a pool of quasi-thermalized electrons with decreased energy (E* 2band). The depopulation kinetics of electrons at E* 2 can be fitted by bi-exponential decay function with lifetimes of 1.7 (± 0.1) ps and 24 (± 2) ps. Different cooling rates of hot electrons at these two excess energy states indicate different cooling dynamic stages.

S9. Calculation of excess energy from TR-2PPE spectrogram

After the complete cooling (both of electrons and optical phonons) at long delay time, the electrons accumulate to the 1S exciton state. The photoelectrons extracted from this state have kinetic energy of roughly 0.95 eV. Therefore, the excess energy equals to kinetic energy minus 0.95 eV. For example, when the average kinetic energy is 1.25 eV, the average excess energy is 0.3 eV.

S10. Initial system energy and fast component analysis for TA results

We can evaluate from the initial excess energy of hot carriers (i.e. 1.1 eV larger than the bandgap under 3.1 eV excitation) what would be the corresponding carrier temperature at time zero. If we assume that the energy is equally distributed between electron and hole, the initial thermal energy of the excited electrons is $E = 1.5\ k_B T = 0.55$ eV giving $T = \sim 4200$ K, which is close to the value adopted from TR-2PPE results as shown in Figure 2c, 3a and 3b.

Using this value and doing the exponential fitting on the HC cooling dynamic for TA analysis, we obtain the upper limit value for the fast component is around 0.1 ps.

In the above discussion, the carriers are assumed can move to other layer (quasi two-dimensional structure). To futher confirm the upper limit of fast component in two-dimensional structure (carriers can't move between layers), the carrier temperature can be calculated from initial thermal enregy $E = k_B T = 0.55$ eV giving $T = \sim 6400$ K.

$$E_{carrier} = 0.55\ eV = k_B \times T \tag{5}$$

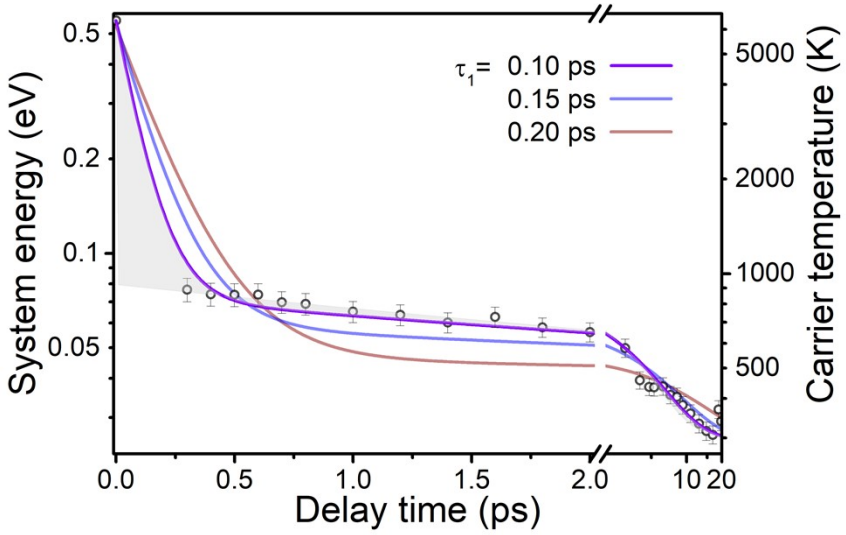

Figure S19. HC temperature kinetic extracted from TA measurements with the initial carrier temperature is assumed to be 6400 K. The kinetic is fitted with bi-exponential function, where the fast component is fixed to be 0.1, 0.15 and 0.2 ps.

Then, we use the 6400 K as the initial data point in Figure S19 and place the bi-exponential fitting on it. It clearly shows that under this circumstance the fast component has shorter timescale than the case in main text. Therefore, the conclusion that 0.1 ps is the upper limit for the fast component in TA analysis is valid.

S11. Low-energy electron diffraction (LEED) measurements

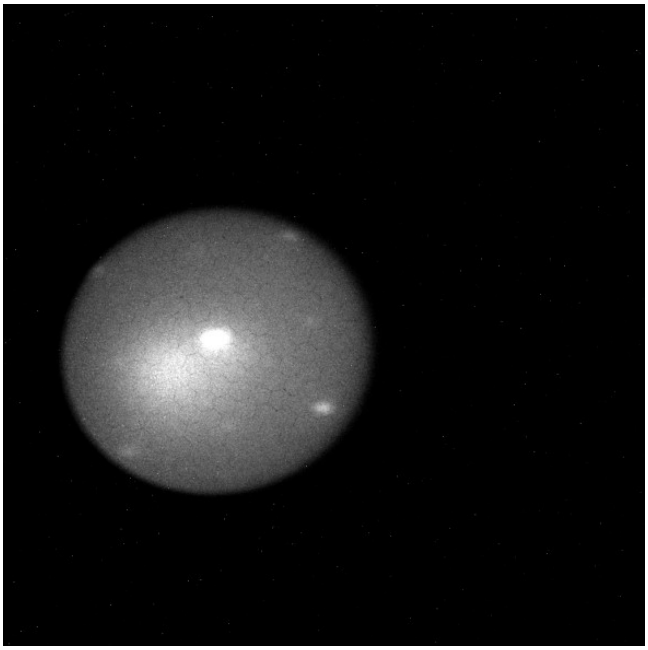

Figure S20. LEED measurements with 4.86 eV of electron kinetic energy.

To have a clearer insight on the mechanism of fast decay within 1 ps in TR-2PPE measurement, the LEED measurement was taken placed to investigate the structure of exposed first layer. The LEED pattern was taken at start voltage of 5 and 10 eV respectively for Figure 4(a) and Figure S20. The kinetic energy was corrected to be 4.86 and 9.86 eV with a small difference of 0.14 eV due to the relation between sample's work function and electron gun's. In Figure 4(a), one can measure the distances from (00) to four (10) spots and the average distance is 212.5 pixels. The average distance from (00) to the Ewald sphere edge (along the same directions from (00) to (01) is 236.5 pixels. As the wavelength of 4.86 eV electron beam is 5.56 Å and then the wave vector from (00) to (01) is 2π / (6.188 Å), by considering the ratio between (00) to Ewald sphere edge and (00) to (01).[c] It means the lattice of the surface atoms that make this LEED should have the lattice vector is 6.188 $\pm$ 0.2 Å, where the error is considered based on the possible 7 pixels error in the measurements.

[c] Calculation of wave vector: $k = \frac{2\pi}{5.56\text{Å} \times 212.5/236.5} = \frac{2\pi}{6.188\text{Å}}$

The distance between Pb atoms is 6.305 Å based on structure stimulation, namely between two Octahedron's centers. The value is the closest one to the number from the LEED measurements and is also consistent with the physical reality that there is no clear inorganic layer distortion on the surface layer.

S12. 2D perovskite flake preparation and position-selective TA measurements

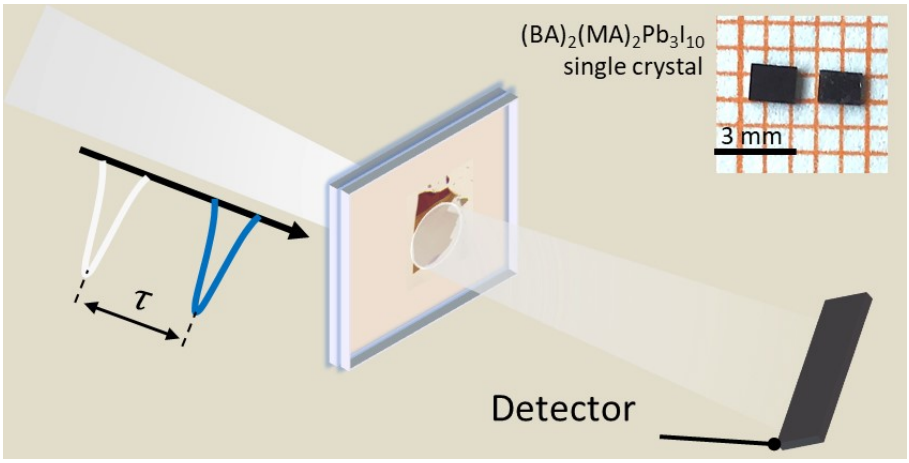

Figure S21. Schematic of encapsulated 2D perovskite flake during TA measurements.

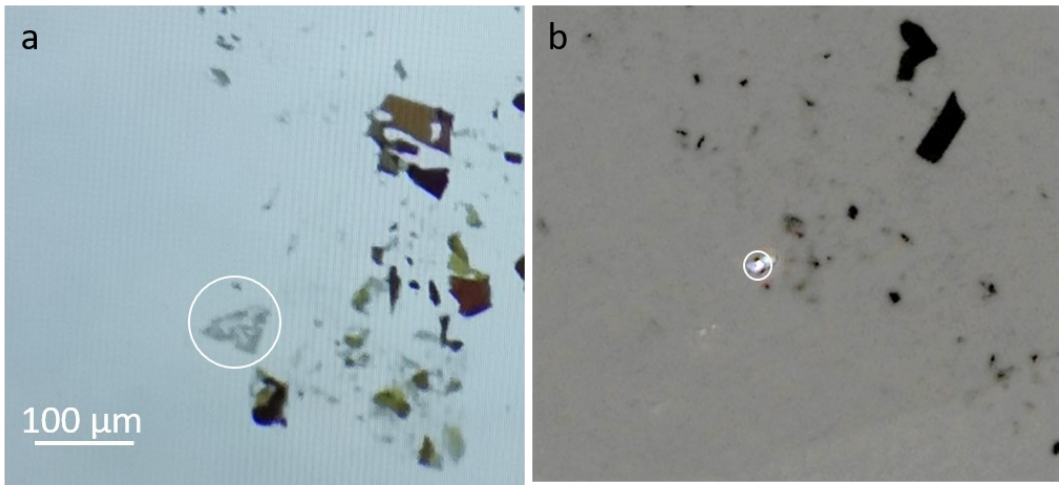

Figure S22. (a) Optical microscope image of flake. (b) Digital microscope image during TA measurements. The white circles represent the probe beam in TA measurements.

S13. Estimation of lattice temperature and hot phonon bottleneck temperature

Under the 3.1 eV excitation, the initial excess energy of the hot carriers is 1.1 eV, by considering the bandgap of 2D perovskite is around 2 eV. When applying 120 μJ/cm^2 per pulse intensity which is used in TA measurements, the carrier density is 2.4 × 10^{19} cm^{-3}. The volume of the chosen unit for 2D perovskite is around 1.1 nm^3. By multiplying with the carrier density, the result turns out that we have 2.64 × 10^{-2} carrier per unit cell. Therefore, the total energy contained in one unit cell will be 0.029 eV. Considering the formula of 2D perovskite as $(BA)_2(MA)_2Pb_3I_{10}$, there are 17 parts (two BA, two MA, three Pb atom and ten I atom) in one unit cell. The number of degrees of freedom is 17 × 3. Assuming that all energy is transferred to the lattice, the total increase of the lattice temperature is 6 K based on eq 3.
The calculation implies that after the final equilibration the lattice is unlikely to achieve high temperature in our study.

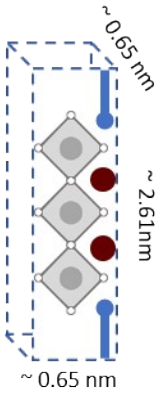

Figure S23. Volume estimation of one $(BA)_2(MA)_2Pb_3I_{10}$ crystal unit, where the blue parts represent the spacing cation, red parts represent MA cation, and the grey parts represent the inorganic octahedra.

$$\varepsilon = 2.303 \times A/d \tag{6}$$

In the envisioned cooling process initially the electron energy would be given to a single degree of freedom of the unit cell corresponding to the LO phonon. This allows to estimate the hot phonon bottleneck temperature as ambient temperature plus the temperature rise from photoexcitation (0.029 eV = k_B × 340 K). The calculation gives hot phonon bottleneck temperature as 640 K in TA measurement and 475 K in TR-2PPE measurement, which agree with the experimental results as 900 K in TA measurement and 480 K in TR-2PPE measurement shown in Figure 3a. More work is needed for drawing further conclusions regarding the cooling details.

S14. Calculation of binding energy based on temperature dependent photoluminescence measurements

The temperature dependent PL spectra were measured on 2D perovskite sample in a cryostat cooled with liquid nitrogen under an excitation wavelength of 375 nm.

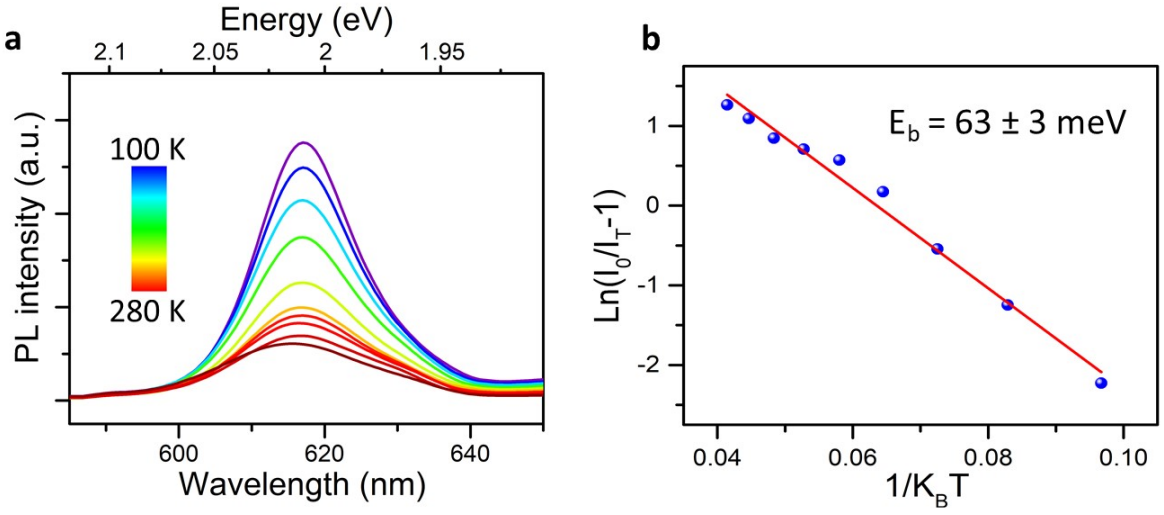

Figure S24. (a) The temperature dependent PL spectra of 2D perovskite at temperature from 100 to 280 K and (b) ln(I_0/I(T)-1) vs 1/k_BT plot of temperature dependent PL spectra.

Since the PL intensity decreases with temperature increasing due to the thermal dissociation of excitons at high temperatures, the temperature dependence trend of PL intensity I(T) can be fitted with

$$I(T) = \frac{I_0}{1 + Ae^{(-E_b/k_BT)}} \quad (7)$$

where the I_0 is the PL intensity at low temperature nad E_b is the binding energy. By fitting the ln(I_0/I(T)-1) vs 1/k_BT plot with linear function, the value of binding energy (around 60 meV) can be obtained as the slope.

References

1 M. Liang, W. Lin, Q. Zhao, X. Zou, Z. Lan, J. Meng, Q. Shi, I. E. Castelli, S. E. Canton, T. Pullerits and K. Zheng, *J. Phys. Chem. Lett.*, 2021, **12**, 4965-4971.

2 J. Faure, J. Mauchain, E. Papalazarou, W. Yan, J. Pinon, M. Marsi and L. Perfetti, *Rev. Sci. Instrum.*, 2012, **83**, 043109.

3 J. Fu, Q. Xu, G. Han, B. Wu, C. H. A. Huan, M. L. Leek and T. C. Sum, *Nat. Commun.*, 2017, **8**, 1300.

4 J. Yang, X. Wen, H. Xia, R. Sheng, Q. Ma, J. Kim, P. Tapping, T. Harada, T. W. Kee, F. Huang, Y. B. Cheng, M. Green, A. Ho-Baillie, S. Huang, S. Shrestha, R. Patterson and G. Conibeer, *Nat. Commun.*, 2017, **8**, 14120.

Author Contributions

T. P., K. Z. and S. C. conceived and supervised the whole project. W. L. and M. L. implemented the sample preparation, performed the experiments and analyzed the data. Y. N. performed the LEED measurements and analyzed the data. W. L., M. L., Z. C. and M. C. performed the TR-2PPE measurements under the supervision of E. P., L. P. and M. M. J. M., X. Z. and Q. Z. helped with optical measurements. J. M. and H. G. helped with TA data analyses. W. L. and L. P. performed TR-2PPE fitting. W. L. wrote the manuscript. M. L., Y. N., Z. C., M. M., L. P., S. C., K. Z. and T. P. provided revisions to the manuscript. All authors commented the manuscript and gave approval to the final submitted version of the manuscript. +W. L. and M. L. contributed equally to this work.